HOKKAIDO UNIVERSITY

Title	Lateral tunneling injection and peripheral dynamic charging in nanometer-scale Schottky gates on AlGaN/GaN hetrosturucture transistors
Author(s)	Kotani, Junji; Kasai, Seiya; 葛西, 誠也 et al.
Citation	Journal of Vacuum Science & Technology B: Microelectronics and Nanometer Structures, 23(4), 1799-1807 https://doi.org/10.1116/1.1942507
Issue Date	2005-07
Doc URL	https://hdl.handle.net/2115/5549
Rights	Copyright © 2005 American Institute of Physics
Type	journal article
File Information	JVSTB23-4.pdf

Hokkaido University Collection of Scholarly and Academic Papers : HUSCAP

Lateral tunneling injection and peripheral dynamic charging in nanometer-scale Schottky gates on AlGaN/GaN hetrosturucture transistors

Junji Kotani,[a] Seiya Kasai, Tamotsu Hashizume, and Hideki Hasegawa
Research Center for Integrated Quantum Electronics (RCIQE) and Graduate School of Information Science and Technology, Hokkaido University, Sapporo, 060-8628, Japan

(Received 23 January 2005; accepted 26 February 2005; published 25 July 2005)

The gate leakage and gate control characteristics of AlGaN/GaN heterostructure field effect transistors (HFETs) were systematically investigated in an attempt to clarify possible effects of surface states. The experiments were compared to rigorous computer simulations. We observed large amounts of leakage currents in the Schottky diodes fabricated on the AlGaN epitaxial layers. By the calculation based on a thin surface barrier model in which the effects of surface defect donor were taken into account, this large leakage was well explained by enhancement of tunneling transport processes due to the barrier thinning associated with ionization of surface-defect donor. On the other hand, the analysis on the current-voltage characteristics for the nanometer-scale Schottky contacts on AlGaN/GaN HFETs, indicated additional lateral leakage components. The comparison of the gate control characteristics between experiment and calculation clearly showed that the effective lateral expansion of gate length significantly impeded the g_m enhancement by the reduction of geometrical gate length. This can be explained by the lateral electron tunneling process at the AlGaN surface stimulated by the pronounced gate leakage currents. Due to frequent tunneling transfer at the gate periphery, surface state occupancy near the gate becomes governed by the metal Fermi level, causing the dynamic surface state charging effects. This resulted in effective widening of the gate length, leading to degradation of gate control performance in AlGaN/GaN HFETs. © *2005 American Vacuum Society.* [DOI: 10.1116/1.1942507]

I. INTRODUCTION

Although significant progress has been achieved in the GaN-based high-power/high-frequency electronic devices such as AlGaN/GaN heterostructure field effect transistors (HFETs), surface-related problems still need an immediate solution. Large leakage currents through Schottky contacts and the drain current collapse not only impede device reliability but also degrade power efficiency and noise performance in GaN-based devices. In addition, it is known that the cut-off frequency f_T of the AlGaN/GaN HFETs starts to largely deviate from dependence of inverse of gate length ($1/L_G$) and quickly saturates to an unexpectedly small value.

Schottky diodes formed on GaN and AlGaN are suffering from serious reverse leakage currents that are many orders of magnitude lager than the prediction of the thermionic emission (TE) model.[1–6] The leakage problem becomes more severe under high-power operation of HFETs, because the device temperature can become as high as 150 °C.[7] Miller, Dang, and Yu[2] discussed the leakage mechanism in AlGaN Schottky interfaces on the basis of the field-emission (FE) tunneling transport assuming a triangular Schottky potential. However, unreasonably higher donor densities than the actual doping concentration were required in their calculation for reproduction of the experimental data. Karmalkar, Sathaiya, and Shur[8] suggested the trap-assisted tunneling model to explain the leakage mechanism in the reverse bias region. However, such a model requires an unlikely defect continuum with a wide energy band throughout a depletion region in semiconductor. Hasegawa and Oyama[4] and Kotani, Hashizume, and Hasegawa[9] have recently proposed the thin surface barrier (TSB) model for the current transport mechanism in GaN and AlGaN Schottky barriers. By using a rigorous simulation method taking account of the effects of nitrogen-vacancy (V_N) related deep donor level, various experimental current-voltage (I-V) characteristics of the GaN and AlGaN Schottky diodes were explained for both forward and reverse biases at different temperatures. Thus, they revealed that enhancement of the tunneling transport processes by the barrier thinning due to the processing-induced V_N-related defect donor is the dominant mechanism associated with large leakage currents through GaN and AlGaN Schottky interfaces.[9]

The current collapse effects have often been observed AlGaN/GaN HFETs under quiescent gate stress[10] or pulse-mode gate stress.[11,12] The collapse is also induced by drain stress.[13,14] Hasegawa and coworkers[5] explained that the charging effects of the surface electronic states, consisting of a U-shaped surface state continuum and V_N-related near-surface deep donor, play a dominant role for the current collapse,[5] as schematically shown in Fig. 1. The injection of high-energy electrons takes place from the two-dimensional electron gas (2DEG) channel into the AlGaN region near the drain edge under the application of a large drain stress, leading to the current collapse.[5] Thus, the surface-related effects are greatly associated with performance and reliability degradation in GaN-based electron devices.

[a]Author to whom correspondence should be addressed; electronic mail: kotani@rciqe.hokudai.ac.jp

 0734-211X/2005/23(4)/1799/9/$22.00 ©2005 American Vacuum Society

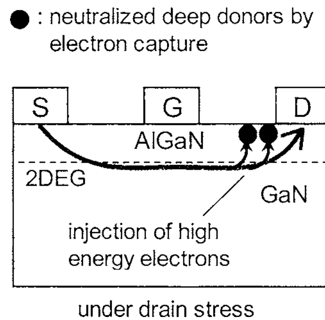

FIG. 1. Schematic illustration of the proposed model for mechanism of current collapse in AlGaN/GaN HFETs (Ref. 5).

Figure 2 shows the reported f_T data as a function of the gate length for the InP- and GaN-based HFETs.[15–21] The f_T saturation in the AlGaN/GaN HFETs appears even at the gate length of around 200 nm that is longer than that of the InP HFETs. Although this significantly impedes the devices working at higher frequencies with the reduction of the gate length, its mechanism is not understood yet.

The purpose of this article is to investigate the current-voltage characteristics and gate control characteristics of nanometer-scale Schottky gates formed on planar AlGaN/GaN HFETs in an attempt to clarify possible effects of surface states.

II. EXPERIMENTAL AND THEORETICAL APPROACHES

A. Sample structures and fabrication process

Figures 3(a) and 3(b) show schematic illustrations of AlGaN and AlGaN/GaN sample structures, respectively, used in this study. High-quality Si-doped $Al_{0.26}Ga_{0.74}N$ layers grown on sapphire substrates by metal organic vapor phase epitaxy (MOVPE) were used in this study. Typical values of electron concentration and mobility of the Si-doped layer at room temperature (RT) is 3×10^{17} cm^{-3} and 100 cm^2/Vs, respectively. The AlGaN/GaN heterostructure samples were also grown by MOVPE. The n-AlGaN layer was doped with Si (2×10^{18} cm^{-3}), while the top and spacer

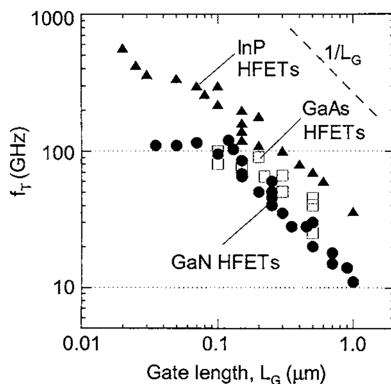

FIG. 2. Plots of cut-off frequency f_T as a function of gate length L_G for InP- and GaN-based HFETs.

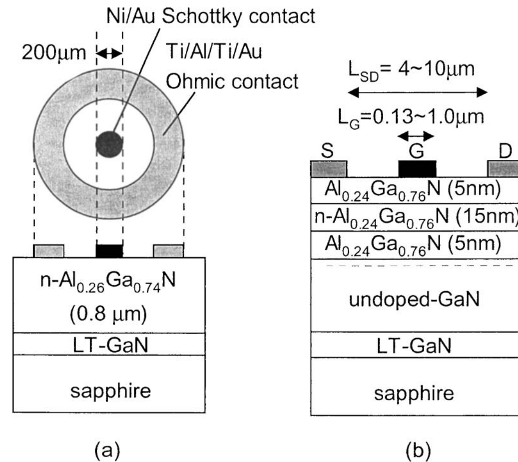

FIG. 3. Schematic illustrations of sample structures for (a) a Schottky diode on thick AlGaN layer and (b) AlGaN/GaN HFETs.

AlGaN layers were ones without doping, as shown in Fig. 3(b). The Al content in AlGaN is 0.24. Typical values of the electron concentration and mobility of (2DEG) at RT were 1.0×10^{13} cm^{-2} and 1100 cm^2/Vs, respectively.

As the start of the sample fabrication process, the sample surface was subjected to a wet chemical treatment in an NH_4OH solution at 50 °C for 5–10 min after conventional cleaning in organic solvents at RT. The treatment in an NH_4OH solution is effective in reducing natural oxides on AlGaN surfaces.[22] For *I-V* measurements of Schottky contacts, circular Ni/Au diode structures with a diameter of 200 μm, as shown in Fig. 3(a), were formed on the AlGaN layer by electron-beam deposition. As a ring-shape ohmic contact, a Ti/Al/Ti/Au layer structure was deposited on the AlGaN surface followed by the annealing at 800 °C for 1 min in N_2 ambient.

For HFET fabrication, an isolation process was carried out using an electron-cyclotron resonance -assisted reactive ion beam etching using a CH_4-based gas system consisting of CH_4, H_2, Ar, and N_2. The addition of N_2 to the gas system is very effective in achieving a smooth and stoichiometric surface.[23] The Ti/Al/Ti/Au ohmic contacts were also used for source and drain electrodes. The Ni/Au gate patterns were defined and fabricated by a combination of electron-beam lithography and lift-off techniques. The gate width W_G was fixed at 60 μm, while the gate length L_G ranged from 130 to 1000 nm. We fabricated the HFETs with the drain-source spacings of 4, 6, and 10 μm. No surface passivation was applied to all the devices fabricated.

B. Computer simulation of current transport in Schottky barriers

We have developed a one-dimensional simulation method for the calculation of current through Schottky interface based on the thin surface barrier (TSB) model,[4,9] as schematically shown in Fig. 4. This model assumes the unintentional introduction of high density of defect donors near GaN or AlGaN surfaces, which reduces the width of the Schottky

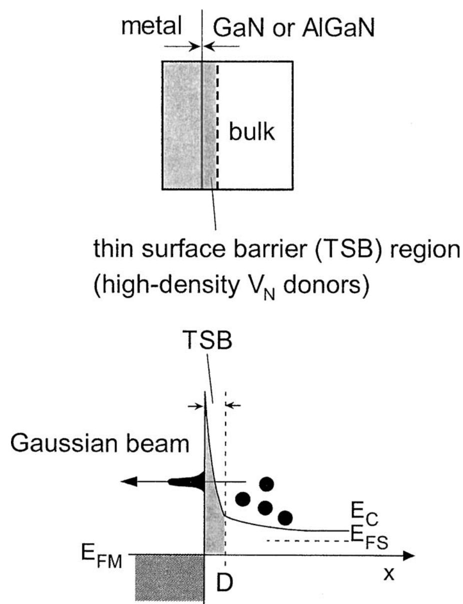

FIG. 4. Thin surface barrier (TSB) model.

barrier in such a way that electrons can tunnel though this barrier in both forward and reverse directions.

The current J from semiconductor to metal through the Schottky barrier can be expressed by the following general expression:[9]

$$J = \frac{4\pi q m^*}{h^3}\int_0^\infty T(E_x)\int_0^\infty [f_s(E_p+E_x) - f_m(E_p+E_x)]dE_p dE_x, \quad (1)$$

where m^* is the effective mass, h is the Plank constant, $T(E_x)$ is the tunneling probability, E_x and E_p are the energy components normal and parallel to the Schottky barrier, respectively, and $f_s(E)$ and $f_m(E)$ are the Fermi-Dirac distribution functions for semiconductor and metal, respectively. Here, it is assumed that the wave numbers parallel to the barrier are conserved during tunneling. $T\ (E_x)$ was calculated using the Wentzel-Kramers-Brillouin (WKB) approximation

$$T(E_x) = \exp\left[-2\frac{\sqrt{2m^*}}{\hbar}\int_{x_1}^{x_2}\sqrt{\phi(x) - E_x dx}\right], \quad (2)$$

where $\phi(x)$ is the potential distribution and x_1 and x_2 are classical turning points.

We first calculated the potential profile of the Schottky interface by solving the Poisson's equation self-consistently, taking account of the surface defect donor with an arbitrary spatial distribution in density. Then the currents through the Schottky interface were calculated using Eqs. (1) and (2) for both forward and reverse bias voltages at different temperatures. Thus the present method is applicable to any Schottky interfaces with arbitrary potential shapes.

We proposed in our previous article[5] that the defect donor is due to N vacancy or its related complex. Theoretical calculations proposed that a simple N vacancy defect (V_N) acts as a shallow donor[24,25] or a s-like deep donor.[26] Experimentally, our recent study detected presence of a N-vacancy related deep donor level[5] with the energy depth of 0.37 eV on the $Al_{0.28}Ga_{0.72}N$ surface. Thus, V_N or its complex was considered to be the most possible candidate for the surface defect donor.

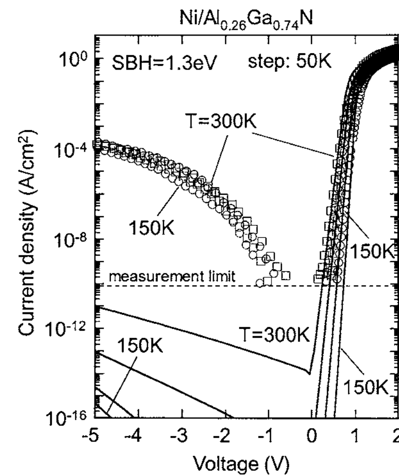

FIG. 5. Measured and calculated *I-V-T* characteristics of the Schottky diodes fabricated on the $Al_{0.26}Ga_{0.74}N$ layer. The measured temperatures were 150, 200, 250, and 300 K. Calculation was carried out without assuming the surface defect donor. Series resistances were considered in the calculation.

C. Computer simulation of gate control characteristics

To investigate gate controllability of AlGaN/GaN HFETs, we calculated drain current at small drain bias region using a computer program that solved a two-dimensional (2D) Poisson's equation by a successive over relaxation method. In the calculation, the 2DEG density and the quantized energy at heterointerface were taken into account, and they were calculated self-consistently with the potential. The surface Fermi level of AlGaN was assumed completely pinned at -1.3 eV from E_C, corresponding to the charge neutrality level given by the disorder-gap state model[27] and the branch point data.[28] In fact, x-ray photoelectron spectroscopy analysis[29] showed the pinning position of 1.33 eV for the surface of $Al_{0.4}Ga_{0.6}N$. The current was calculated using a simple drain current formula for FETs in the linear region including the effect of a series resistance.

III. EXPERIMENTAL RESULTS

A. *I-V* characteristics of Schottky diodes on thick AlGaN layers

Figure 5 shows measured and calculated *I-V-T* characteristics of the Schottky diodes fabricated on the $Al_{0.26}Ga_{0.74}N$ layer. If we pay attention only to the forward current at room temperature (RT), the *I-V* behavior apparently follows the simple TE or TFE transport model. To investigate this, we calculated the *I-V* curves without assuming the surface defect donor. The calculated results are shown in solid lines in Fig. 5. A large deviation between experiment and calculation was seen. In particular, we found that the experimental tem-

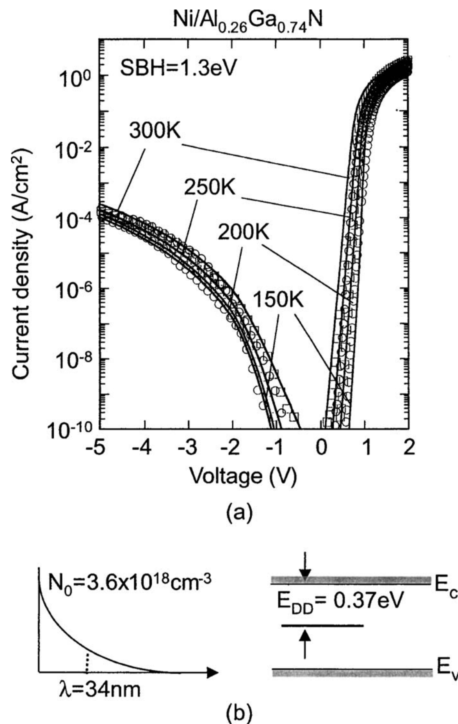

FIG. 6. (a) Measured and calculated *I-V-T* characteristics of the Schottky diodes fabricated on the $Al_{0.26}Ga_{0.74}N$ layer. The effects of the V_N-related donor level were taken into account in the calculation. (b) The exponentially decaying density distribution and the energy depth of the V_N-related donor level used in the calculation.

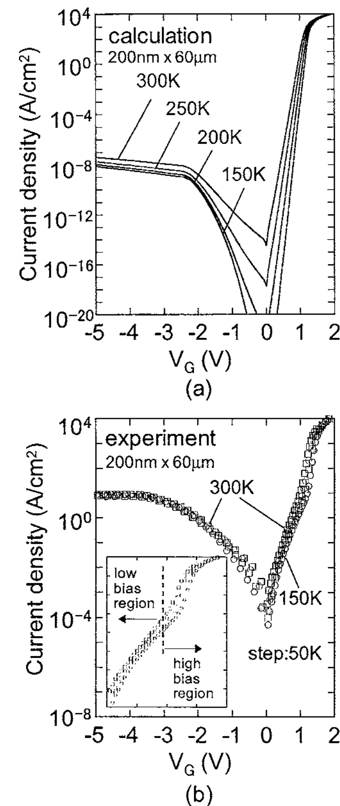

FIG. 7. (a) Calculated *I-V-T* curves of the Schottky gates fabricated on AlGaN/GaN HFET structures without assuming surface donor defect. The gate size is 200 nm × 60 μm. (b) Measured *I-V-T* curves at 150, 200, 250, and 300 K. The change in slope of *I-V* curve for the forward bias region is indicated in the inset.

perature dependence of *I-V* curves was surprisingly small and that leakage currents were anomalously large in the reverse bias region.

Then we applied our simulation method to fit the experimental data, taking account of the V_N-related donor level. After many trials, we obtained the best fitting result for the Ni/AlGaN Schottky diode, as indicated by the solid lines in Fig. 6(a). It is noted that series resistances were considered in the calculation. To achieve such good fitting for both forward and reverse directions simultaneously, we found that defect donors should have specific features. Namely, the experimental data could be reproduced only by assuming that the defect donor is a deep donor with an exponentially decaying spatial distribution shown in Fig. 6(b). The energy depth from the bottom of the conduction band E_{DD} should be 0.37 eV, corresponding to an experimentally obtained value.[5] The net sheet density of the V_N-related donor was predicted to be 1.2×10^{13} cm^{-2}. Such exponentially decaying spatial distribution with high density indicated that the V_N-related donor defect could be introduced to the AlGaN surface during the electron beam (EB)-deposition process of metals where the surface was hit by high-energy metal atoms.[9] The enhancement of tunneling transport processes by the barrier thinning due to the processing-induced V_N-related defect seems to be the dominant mechanism associated with large leakage currents through AlGaN Schottky interfaces.

B. Leakage characteristics of nanometer-scale Schottky gate on AlGaN/GaN HFETs

Next, we investigated *I-V* characteristics of the Schottky gates fabricated on AlGaN/GaN HFET structures. The gate length and the drain-source spacing were 200 nm and 6.0 μm, respectively. First, we calculated the *I-V* curves without assuming surface donor defect. As indicated by the solid lines in Fig. 7(a), the calculation showed the saturation behavior of reverse leakage current due to the depletion of 2DEG under the Schottky gate. The temperature dependence of *I-V* curves is expectedly seen in the calculated result for both forward and reverse biases.

However, the experimental *I-V* curves in Fig. 7(b) exhibited completely different behavior with the theoretical prediction. It is noted that a vertical scale in Fig. 7(b) is different from that in Fig. 7(a). For both forward and reverse bias voltages, the magnitude of the experimental current was far larger than the calculated one, and the extremely less temperature dependence of currents was observed.

Based on the successful fitting results on the Schottky diode fabricated on thick AlGaN layers as well as various types of GaN Schottky diodes,[9] we tried to fit the experimental *I-V* data using our simulation with taking the defect donor into account. We assumed an exponentially decaying distribution and an energy depth of E_C-0.37 eV for the V_N-related

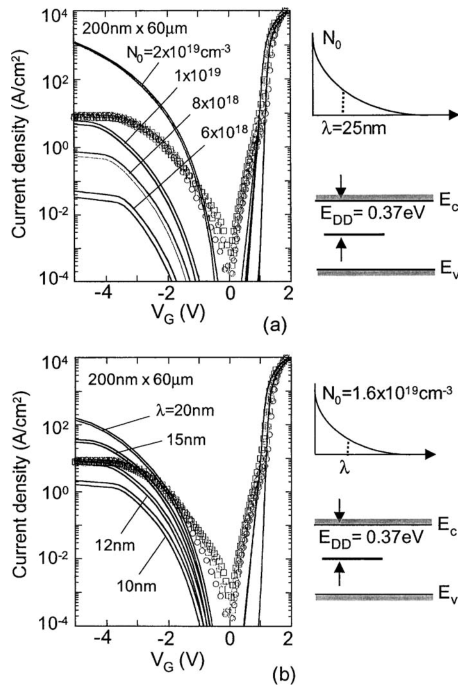

FIG. 8. Comparison of *I-V-T* curves of the Schottky gates fabricated on AlGaN/GaN HFET structures between experiment and calculation for (a) fixed decaying depth and (b) fixed density of the V_N-related donor level. The Schottky barrier height used in the calculation was 1.4 eV.

defect donor level, as used in the calculation for the AlGaN Schottky diode. Figure 8(a) shows a set of calculated results together with the experimental data. In this case, we fixed the characteristic decay depth of 25 nm, corresponding to the total thickness of the AlGaN barrier layer in the AlGaN/GaN heterostructure. The reverse leakage currents increase with the density of the V_N defect donor, again due to the enhancement of the tunneling transport process by the barrier thinning with ionization of the V_N defect donor. However, the temperature and reverse-bias dependences on current are completely different between experiment and calculation. For the low bias region, in addition, the calculated currents showed much lower values than the experimental ones at given temperatures even when an extremely high density of the V_N-related donor was introduced to AlGaN barrier layer, as shown in Fig. 8(a).

Next, we carried out the calculation with a condition of the fixed defect concentration of 1.5×10^{19} cm^{-3}. The result is shown in Fig. 8(b). A relatively good agreement between experiment and calculation was obtained in high forward bias region. In the case of $\lambda = 12$ nm, in addition, the calculation showed a similar current level to experiment at the pinch-off region for the reverse bias. However, the calculated currents were much lower than the experimental ones at low voltage region for both forward and reverse biases. We have tried to fit the experimental *I-V-T* curves using various kinds of density distributions of the V_N-related defect donor. In any cases, however, the calculation could not reproduce the experimental *I-V* curves of the Schottky gates fabricated on AlGaN/GaN HFET structures, in spite of the fact that the

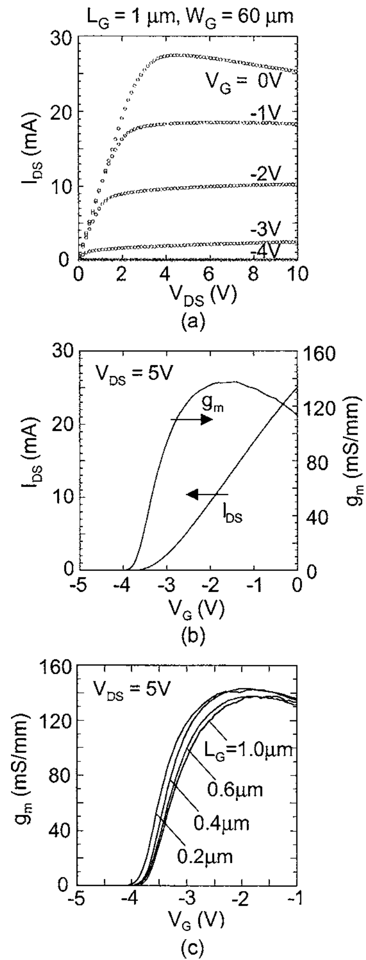

FIG. 9. (a) Typical drain *I-V* characteristics and (b) the transfer characteristics of the fabricated AlGaN/GaN HFET with a gate length of 1.0 μm and a drain-gate spacing of 4.0 μm. (c) The transfer characteristics of the devices with L_G ranging from 200 to 1000 nm.

present simulation is a powerful tool to fit *I-V* characteristics of various kinds of Schottky diodes fabricated on GaN and AlGaN thick layers.

Thus, the results obtained strongly indicated that the leakage mechanism of the nanometer-scale Schottky gates fabricated on the AlGaN/GaN was different from that in Schottky diodes with larger sizes fabricated on thick AlGaN layers.

C. DC characteristics of AlGaN/GaN HFETs

Figure 9(a) shows a typical drain *I-V* characteristics of the fabricated AlGaN/GaN HFET with a gate length of 1.0 μm and a drain-gate spacing of 4.0 μm. Good saturation and pinch-off behavior were observed, although a heating effect appeared in higher drain voltages at V_G=0 V. The transfer characteristics are shown in Fig. 9(b). The device exhibited an excellent linearity and a maximum value of transconductance g_m of 130 mS/mm.

To investigate gate control characteristics of the Schottky gates, we measured the transfer characteristics of the devices with L_G ranging from 200 to 1000 nm. The result at V_{DS} =5 V is shown in Fig. 9(c). Although the $g_m$value slightly

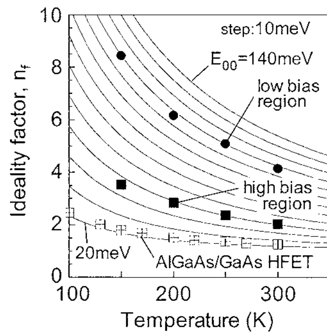

FIG. 10. Plots of n_F values as a function of temperature. The n_F values were separately obtained from two slopes of the *I-V* curve at low and high bias regions, as indicated in the inset in Fig. 7(b). The calculated curves with E_{00} from 20 to 140 meV are also shown by the solid lines.

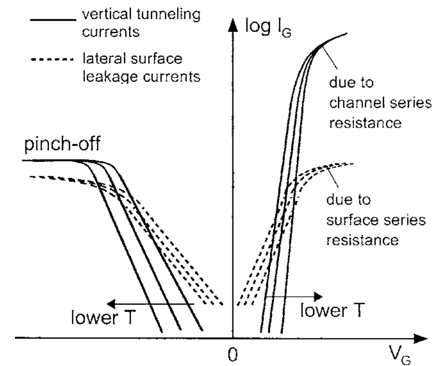

FIG. 11. Schematic illustration for qualitatively explaining the observed *I-V-T* characteristics for the nanometer-scale Schottky contacts on AlGaM/GaN heterostructure.

increased with reducing L_G from 1000 to 400 nm, it was saturated for $L_G < 400$ nm. One might suppose the so-called short-channel effects. However, they basically appear when the aspect ratio of the gate length to the gate-channel distance falls below 5 in the HFET devices.[30–32] Thus, it was unlikely that the apparent saturation in g_m indicated the short-channel effects in the AlGaN/GaN HFETs, because the aspect ratio ranged from 8 (L_G=200 nm) to 40 (L_G =1000 nm).

IV. DISCUSSION

We observed large leakage currents for Schottky contacts fabricated on both thick AlGaN layers and AlGaN/GaN heterostructures. Our 1D computer simulation including the defect donor effects could reproduce the experimental *I-V* curves of the Schottky contacts with a large area on thick AlGaN layer, as shown in Fig. 6. This indicates that enhancement of tunneling transport perpendicular to the Schottky interface is dominant in the leakage mechanism, due to ionization of the V_N-related donor level. However, this is not the case for the nanometer-scale Schottky contacts on the AlGaN/GaN heterostructures. The 1D simulation could not show a reasonable agreement with the experimental *I-V* data for the Schottky contacts on AlGaN/GaN, indicating an additional leakage process to normal to Schottky interfaces. In addition, an expected gate control characteristics did not appear in the AlGaN/GaN HFETs with nanometer-scale Schottky gates, as shown in Fig. 9(c).

To further investigate the leakage characteristics of nanometer-scale Schottky gates on the AlGaN/GaN HFETs, the temperature dependence of the ideality factor for forward current was analyzed. In the case of the forward currents, the transport is mainly the TFE mechanism and the ideality factor for forward currents n_F is given by the following formula.[33]

$$n_F = \frac{E_{00}}{kT}\coth\left(\frac{E_{00}}{kT}\right) \tag{3a}$$

$$\text{with } E_{00} = (qh/4\pi)(N_D/m^*\varepsilon_s)^{1/2}, \tag{3b}$$

where q is the electronic charge, h is Planck constant, m^* is the effective mass, ε_s is the permittivity of semiconductor, and N_D is the donor density. As indicated in the inset of Fig. 7(b), we observed the change in slope of *I-V* curve at the forward bias region. Therefore, we obtained separate n_F values from each slope of *I-V* curves at different temperatures.

The measured values of n_F are compared in Fig. 10 with the theoretical curves calculated from Eqs. (3a) and (3b). For comparison, the n_F values obtained from the AlGaAs/GaAs HFET[34] are also plotted in Fig. 10. The measured values of n_F could be very well fitted into the theoretical curves. The E_{00} values estimated from the plots in Fig. 10 were 50 and 110 meV for the high and low bias regions, respectively. These are much higher than that of the AlGaAs/GaAs HFETs. The corresponding donor concentrations are 1.6×10^{19} and 8.0×10^{19} cm^{-3}, which are far larger than the value of the doping concentration of $N_D = 2 \times 10^{18}$ cm^{-3} in the AlGaN barrier layer. The former value probably indicates the density of the V_N-related donor level, because the calculation using the density around 1×10^{19} cm^{-3} for the V_N-related donor level produced similar leakage current level to experimental one near pinch-off region, as shown in Fig. 8. On the other hand, an unlikely high donor density of 8.0×10^{19} cm^{-3} estimated from the n_F analysis at low forward bias region indicates an additional leakage process to normal to Schottky interfaces, probably lateral leakage pass at the AlGaN surface near the gate edge.

Figure 11 shows a schematic illustration for qualitatively explaining the observed *I-V-T* characteristics for the nanometer-scale Schottky contacts on AlGaN/GaN heterostructure. The solid lines in Fig. 11 indicate the normal vertical currents through the Schottky gate. The transport mechanism of the vertical current component is governed by the tunneling due to the existence of high density of the V_N-related defect donor, and the *I-V-T* characteristics can be reproduced by our simulation method. In addition to the vertical currents, lateral surface leakage currents (broken lines) can flow by an assist of high density of surface states on the AlGaN surface. Due to high impedance of a surface series

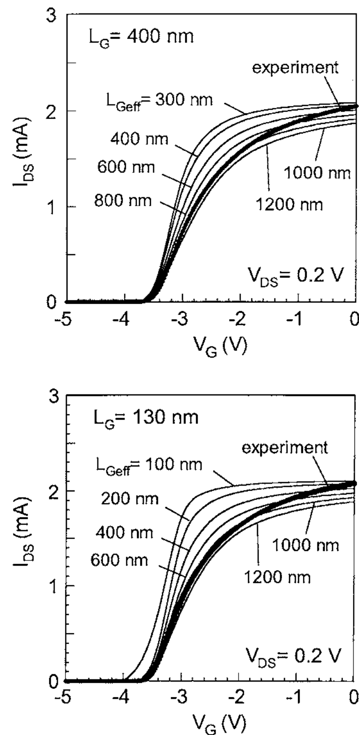

FIG. 12. Measured and calculated $I_{DS}-V_G$ characteristics of AlGaN/GaN HFETs with (a) L_G=130 nm and (b) L_G=400 nm.

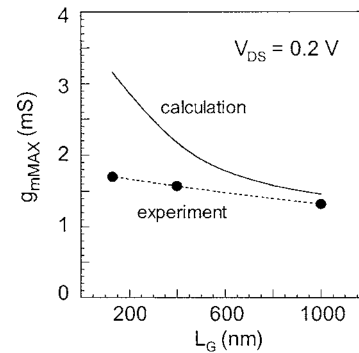

FIG. 13. Measured and calculated maximum values of the transconductances, g_{mMAX}, as a function of gate length.

resistance, the lateral leakage currents may be saturated at a relatively lower current level, leading to change in slope of the *I-V* curve at forward bias. At reverse bias, the lateral leakage currents seem to also be added on the normal vertical currents, and saturation is governed by the pinch off of 2DEG in channel.

To see insight of the gate control characteristics in the fabricated AlGaN/GaN HFETs, the transfer characteristics of the devices having different gate lengths were compared with the calculation. To avoid the complication in the gate potential profile modulation caused by high fields, comparisons were made at a small source-drain bias V_{DS} of 0.2 V. In the calculation, we used the Schottky barrier height of 1.3 eV and the E_F pinning position of E_C-1.3 eV, as previously mentioned.

The measured I_{DS}-V_G characteristics of AlGaN/GaN HFETs with L_G=130 nm and L_G=400 nm were compared with the calculated curves in Figs. 12(a) and 12(b), respectively. For both devices, overall behavior of the measured I_{DS}-V_G characteristics was similar to that of calculated curves. However, the experimental gate-bias dependence of the drain current is much stronger than the theoretical prediction, as shown in Fig. 12. For the device with L_G =130 nm, in particular, the calculation clearly showed the threshold voltage shift due to the expected short-channel effect, while no such shift was observed experimentally. The calculation indicates that the Schottky gates on the fabricated devices effectively act as ones with significantly longer lengths than the geometrical sizes.

Then the maximum values of the transconductances g_{mMAX} are compared with the calculated ones in Fig. 13, as a function of gate length. The calculation predicted the pronounced increase of g_{mMAX}, inversely proportional to the gate length, while only a slight increase was observed experimentally even when the gate length was reduced to 130 nm. The virtual gating effect shown in Fig. 12 could significantly impede the g_m enhancement by the reduction of geometrical gate length.

The effective gate length extension was also observed in GaAs MESFETs and AlGaAs/GaAs HFETs.[35] As mentioned above, large leakage currents can flow in the AlGaN Schottky interfaces by enhancement of tunneling transport process associated with the ionization of a high-density V_N-related deep donor level. In addition, the strong surface Fermi level pinning due to high-density surface states[5] produces large lateral electric field near the gate edge when the negative gate voltages are applied. These enhance the lateral electron tunneling into the AlGaN surface. An excess leakage current appearing in the submicron Schottky gates on the AlGaN/GaN HFETs seems to reflect the lateral carrier injection, as schematically shown in Fig. 14(a). Such lateral tunneling injection can charge up the surface states excessively, and the surface potential becomes higher than that in the thermal-equilibrium condition. In this case, the surface state occupancy near the gate edge is in equilibrium not to the semiconductor Fermi level E_{FS} but to the metal Fermi level E_{FM} as shown in Fig. 14(b). In this regard, the E_{FM}-equilibrium region on the AlGaN surface can appear near the gate edge. Therefore, it acts as a metal gate and extends the effective gate length. The potential can rapidly respond to a gate swing due to strong interaction between charges in a metal and surface states of AlGaN through very thin potential barrier, resulting in the dynamic charging effects. Thus, this virtual gate extension can explain qualitatively the fact that the cut-off frequency f_T starts to largely deviate from the L_G^{-1} scaling and saturates at unexpected small values in the AlGaN/GaN HFETs as shown in Fig. 2. A similar gate periphery effect was also reported in the InP-based HFETs.[31]

Here, it should also be mentioned that lateral leakage current also travels to the drain along the surface and has a

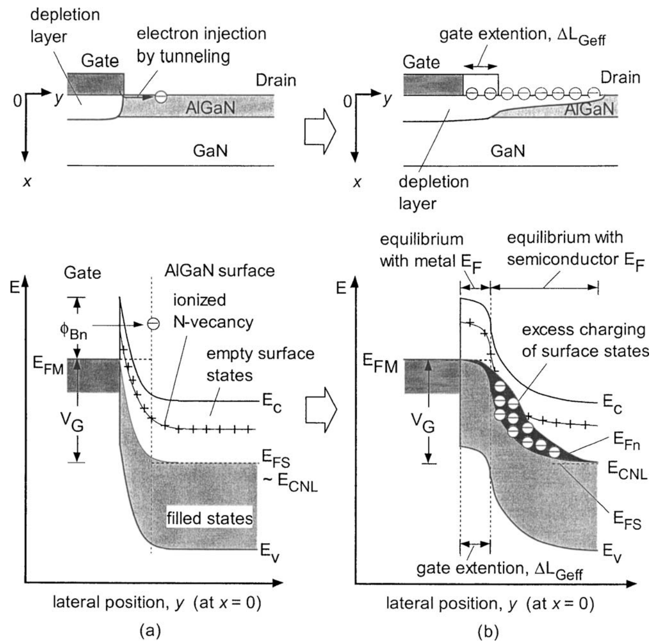

FIG. 14. Model for lateral tunneling injection and gate extension effects near gate edge on AlGaN surface.

chance to fill the acceptorlike surface states in which Fermi level is in equilibrium to that in the semiconductor E_{FS} as shown in Fig. 14(b). The negatively charged surface states also rise the surface potential and deplete the carriers in the 2DEG channel, resulting in the increase of the channel series resistance, the decrease of current, and so on. In this case, the states are spatially far away from the gate edge, and the process through the leakage current may have slower charging/discharging times. In the present study, the observed gate extension behavior included both the dynamic and static lateral surface charging effects, since the gate-control characteristics in HFETs were investigated by dc measurements. However, further quantitative investigation is necessary to reveal the mechanism of the gate extension effects. The results obtained indicate that it is extremely important to suppress the gate leakage problems for improvement of both dc and rf performances of the AlGaN/GaN HFETs.

V. CONCLUSION

We have systematically investigated the gate leakage and gate control characteristics of AlGaN/GaN HFETs in an attempt to clarify possible effects of surface states. The experiments were compared to rigorous computer simulations. We observed large amounts of leakage currents in the Schottky diodes fabricated on the AlGaN epitaxial layers. By the calculation based on a thin surface barrier model in which the effects of surface defect donor were taken into account, this large leakage was well explained by the enhancement of tunneling transport processes due to the barrier thinning associated with ionization of V_N-related defect donor. On the other hand, the analysis on the current-voltage characteristics for the nanometer-scale Schottky contacts on AlGaN/GaN HFETs, indicated an additional lateral leakage component. The comparison of the gate control characteristics between experiment and calculation clearly showed the effective lateral extension of gate length. The effective gate length expansion significantly impeded the g_m enhancement by the reduction of geometrical gate length. This can be explained by the lateral electron tunneling process at the AlGaN surface stimulated by the pronounced gate leakage currents. Due to frequent tunneling transfer at the gate periphery, surface state occupancy near the gate becomes governed by the metal Fermi level, causing the dynamic surface state charging effects. This resulted in effective widening of the gate length, leading to degradation of gate control performance in AlGaN/GaN HFETs. The results obtained indicate that it is extremely important to suppress the gate leakage problems for improvement of both DC and RF performances of the AlGaN/GaN HFETs.

ACKNOWLEDGMENT

This work is supported in part by the 21 Century COE program of "Meme-media technology approach to the R&D of next-generation ITs" from MEXT, Japan.

[1] L. S. Yu, Q. Z. Liu, Q. J. Xing, D. J. Qiao, and S. S. Lau, and J. Redwing, J. Appl. Phys. **84**, 2099 (1998).
[2] E. J. Miller, X. Z. Dang, and E. T. Yu, J. Appl. Phys. **88**, 5951 (2000).
[3] S. Mizuno, Y. Ohno, S. Kishimoto, K. Maezawa, and T. Mizutani, Jpn. J. Appl. Phys., Part 1 **41**, 5125 (2002).
[4] H. Hasegawa and S. Oyama, J. Vac. Sci. Technol. B **20**, 1647 (2002).
[5] H. Hasegawa, T. Inagaki, S. Ootomo, and T. Hashizume, J. Vac. Sci. Technol. B **21**, 1844 (2003).
[6] S. L. Rumyantsev, N. Pala, M. S. Shur, R. Gaska, M. E. Levinshtein. M. A. Khan, G. Simin, X. Hu, and J. Yang, J. Appl. Phys. **88**, 6726 (2000).
[7] M. Kuball, J. M. Hayes, M. J. Uren, T. Martin, J. C. H. Birbeck, R. S. Balmer, and B. T. Hughes, IEEE Electron Device Lett. **23**, 7 (2002).
[8] S. Karmalkar, D. M. Sathaiya, and M. S. Shur, Appl. Phys. Lett. **82**, 3976 (2003).
[9] J. Kotani, T. Hashizume, and H. Hasegawa, J. Vac. Sci. Technol. B **22**, 2179 (2004).
[10] T. Mizutani, Y. Ohno, M. Akita, S. Kishimoto, and K. Maezawa, Phys. Status Solidi A **194**, 447 (2002).
[11] B. Luo, J. W. Johnson, J. Kim, R. M. Mahandru, F. Ren, B. P. Gila, A. H. Onstine, C. R. Abernathy, S. J. Pearton, A. G. Baca, R. D. Briggs, R. J. Shul, C. Monier, and J. Han, Appl. Phys. Lett. **80**, 1661 (2002).
[12] G. Koley, V. Tinayak, L. F. Eastman, and M. G. Spencer, IEEE Trans. Electron Devices **50**, 886 (2003).
[13] R. Vetury, N. Q. Zhang, S. Keller, and U. K. Mishra, IEEE Trans. Electron Devices **48**, 560 (2001).
[14] J. A. Mittereder, S. C. Binari, P. B. Klein, J. A. Roussos, D. S. Katzer, D. F. Stom, D. D. Koleske, A. E. Wickenden, and R. L. Henry, Appl. Phys. Lett. **83**, 1650 (2003).
[15] T. Suemitsu, Oyo Butsuri (in Japanese) **69**, 141 (2000).
[16] Y. Yamashita, A. Endoh, K. Shinohara, K. Hikosaka, T. Matsui, S. Hiyamizu, and T. Mimura, IEEE Electron Device Lett. **23**, 573 (2002).
[17] M. Nicvic, N. X. Nguyen, P. Janke, W. S. Wong, P. Hashimoto, L. M. Maccray, and C. Nguyen, Electron. Lett. **36**, 358 (2000).
[18] L. F. Eastman, V. Tlak, J. Smart, B. M. Green, L. M. Chumbes, R. Dimitrov, H. Kim, O. S. Ambacher, N. Weimann, T. Prunty, M. Murphy, W. J. Shaff, and J. R. Shealy, IEEE Trans. Electron Devices **48**, 479 (2001).
[19] J. A. Bardwell, Y. Liu, H. Tang, J. B. Webb, S. J. Rolfe, and J. Lapointe, Electron. Lett. **39**, 654 (2003).
[20] T. Inoue, Y. Ando, K. Kasahara, Y. Okamoto, T. Nakayama, H. Miyamoto, and M. Kuzuhara, IEICE Trans. Electron. **E86-C**, 2065 (2003).
[21] A. Endoh, Y. Yamashita, K. Ikeda, M. Higashiwaki, K. Hikosaka, T. Matsui, S. Hiyamizu, and T. Mimura, Phys. Status Solidi C **0**, 2368 (2003).

[22]T. Hashizume, S. Ootomo, R. Nakasaki, S. Oyama, and M. Kihara, Appl. Phys. Lett. **76**, 2880 (2000).
[23]Z. Jin, T. Hashizume, and H. Hasegawa, Appl. Surf. Sci. **190**, 361 (2002).
[24]J. Neugebauer and C. G. Van de Walle, Phys. Rev. B **50**, 8067 (1994).
[25]P. Boguslauski, E. L. Briggs, and J. Bernholc, Phys. Rev. B **51**, 17255 (1995).
[26]E. Yamaguchi and M. R. Junnarkar, J. Cryst. Growth **189/190**, 570 (1998).
[27]H. Hasegawa and H. Ohno, J. Vac. Sci. Technol. B **4**, 1130 (1986).
[28]T. U. Kampen and W. Mönch, Appl. Surf. Sci. **117/118**, 388 (1997).
[29]A. Rizzi and H. Lueth, Appl. Phys. A: Mater. Sci. Process. **75**, 69 (2002).
[30]Y. Awano, M. Kosugi, K. Kosemura, T. Mimura, and M. Abe, IEEE Trans. Electron Devices **36**, 2260 (1989).
[31]T. Enoki, M. Tomizawa, Y. Ueda, and Y. Ishii, Jpn. J. Appl. Phys., Part 1 **33**, 798 (1994).
[32]E. Sano, Jpn. J. Appl. Phys., Part 1 **42**, 4261 (2003).
[33]F. A. Padovani and R. Stratton, Solid-State Electron. **9**, 695 (1966).
[34]R. Jia, S. Kasai, and H. Hasegawa, Inst. Phys. Conf. Ser. (to be published).
[35]A. Kameda, S. Kasai, T. Sato, and H. Hasegawa, Solid-State Electron. **47**, 323 (2003).